Journal of ELECTRONIC MATERIALS, Vol. 46, No. 7, 2017
DOI: 10.1007/s11664-017-5317-z

Effect of Si Growth Temperature on Fabrication of Si-ZnO Coaxial Nanorod Heterostructure on (100) Si Substrate

IM TAEK YOON,[1,3] HAK DONG CHO,[1] HOON YOUNG CHO,[2] DONG WOOK KWAK,[2] and SEJOON LEE[2]

1.—Quantum Functional Semiconductor Research Center, Dongguk University, Seoul 100-715, Korea. 2.—Department of Physics and Semiconductor Science, Dongguk University, Seoul 100-715, Korea. 3.—e-mail: ityoon@dongguk.edu

The realization and application of optoelectronics, photonics, and sensing, such as in solar diode sensors and photodiodes, which are potentially useful from ultraviolet to infrared light sensing, is dramatically advanced when ZnO is integrated into semiconductor nanostructures, especially when compatible with mature silicon technology. Here, we compare and analyze the fundamental features of the Si-ZnO coaxial nanorod heterostructures (Si@ZnO NRs) grown on semi-insulating (100)-oriented Si substrates at growing temperatures of 500°C, 600°C, 650°C, and 700°C of the Si layer for device applications. ZnO NRs were grown by a vapor phase transport, and Si layers were made by rapid thermal chemical vapor deposition. X-ray diffraction, field emission scanning electron microscopy (FESEM), energy-dispersive x-ray spectroscopy, and Raman experiments showed that ZnO NRs were single crystals with a würtzite structure, while the Si layer was polysilicon with a zincblende structure. Furthermore, FESEM revealed that Si shell thickness of the Si@ZnO NRs increases with increasing growing temperatures of Si from 500°C to 700°C.

Key words: Coaxial nanorod heterostructures, ZnO nanorod, Si layer, chemical vapor deposition

INTRODUCTION

In recent times, semiconductor coaxial nanorod heterostructures (@NRs) have attracted considerable attention because they have enormous potential in reduced electronic and optoelectronic devices.[1–4] The operation of electronic and optoelectronic devices can be enhanced with ultrafine @NRs because the central NRs have one-dimensional (1D) quantum confinement (QC) influences. The manufacture of submicron GaN@ZnO NRs and results for defects were examined.[5] The synthesis of perpendicularly aligned GaN@ZnO NRs and light emitting diodes (LED) use in the ultraviolet (UV) range was studied.[6] 1D ZnO@MgZnO NRs were recently made and investigated.[7] A QC influence exists in ZnO@ZnMgO NRs, where the size of NRs was structured accurately, down to the monolayer limit.[8] In order to show the cause of their improved luminescence, exciton transport in MgZnO@ZnO NRs was reported.[9] On the other hand, nanostructures and heterostructures based on silicon attracted also considerable attention because they have great applications in nano-electrical devices and structure[10–15] and are compatible with mature silicon technology.[2,16] Recently, Si@ZnS, Si@ZnSe bi-axial nanowires (NWs), ZnS@Si@ZnS tri-axial NWs, ZnSe@Si bi-coaxial NWs, Si@SiGe, and Ni-Si@Si heterostructures were studied.[4,17–19] Many researchers have fabricated and investigated the ZnO/Si nanowire core–shell structure (Si nanowire core and ZnO nanowire shell) or ZnO NRs within silicon nanostructures or ZnO nanowire/silicon microrod hybrid architectures (Si nanowire core and ZnO nanowire shell).[20–22] The reason why ZnO was chosen as a pairing with Si is that Si and ZnO are

(Received May 16, 2016; accepted January 13, 2017; published online February 14, 2017)

essential elements with different characteristics and show potential engineering uses, and nanostructured Si and ZnO are the most investigated materials. Coaxial *p–n* heterojunction devices characterize an advantageous structure to increase the boundary region and carrier split-up as a result of the built-in field formed through the junction. Therefore, the coaxial heterostructures consisting of ZnO NRs (*n*-type) and Si (*p*-type) layer could make full use of the intrinsic features of ZnO and Si with increased shell regions and the development of Si-ZnO heterojunctions. However, 1D Si@ZnO NRs have not been studied up to the present. To the best of our knowledge, this is the first manufacture and characterization of Si@ZnO NRs (ZnO NRs core and Si layer shell).

In this report, we compare and analyze the fundamental features of the Si@ZnO NRs on semi-insulating (100)-oriented Si substrates at Si growing temperatures of 500˚C, 600˚C, 650˚C, and 700˚C for device applications.

EXPERIMENTAL

The ZnO NRs were grown on a semi-insulating (100)-oriented Si substrates by vapor-phase transport (VPT) method. Detailed growing procedures of ZnO NRs were described in previous work.[23] Scanning electron microscopy (SEM) imaging shows that the typical lengths and diameters of the deposited NRs obtained are in the range of 27–30 μm and 250–500 nm. Their straight lengths and uniform diameters are with $<1\%$ deviation, respectively. The as-grown ZnO NRs were perpendicularly aligned with the Si substrate over a 2×2 cm^2 area and had basically *n*-type conduction ($N_e \sim 10^{16}$ cm^2). Succeeding the production of ZnO NRs, Si layers were grown by rapid thermal chemical vapor deposition (RTCVD). Detailed growing procedures of Si@ZnO NRs were also described in previous work.[23]

The morphological characteristic and chemical composition of the Si@ZnO NRs were explored by a field emission scanning electron microscopy (FESEM, XL-30 Philips) and energy-dispersive x-ray spectroscopy (EDS). The lattice structure of the Si@ZnO NRs was analyzed by x-ray diffraction (XRD) with a Cu K radiation (λ = 0.154 nm), and high-resolution transmission electron microscopy (HRTEM) and selected area electron diffraction (SAED). A cross section TEM specimen was thinned and polished carefully using diamond foils and ion milling using a Gatan precision ion polishing system (PIPS). The μ-Raman scattering analysis was carried out at room temperature using a 514 nm Ar+ laser line.

RESULTS AND DISCUSSION

Figure 1a, b, c, and d display cross-sectional and in-plane view with discrete scale: SEM images of as-grown ZnO NRs at (a) scale bar: 50 μm (b) 20 μm (c) 10 μm (d) 5 μm. The mean length of as-grown ZnO NRs is $\sim$28 μm. The cross-sectional SEM images in Fig. 1 and the previous studies on the XRD spectra of as-grown ZnO NRs prove that they are single crystal.[23] Figures 2, 3, 4, and 5 show FESEM images in the cross-sectional and in-plane view for the Si@ZnO NRs made at growing temperature of Si

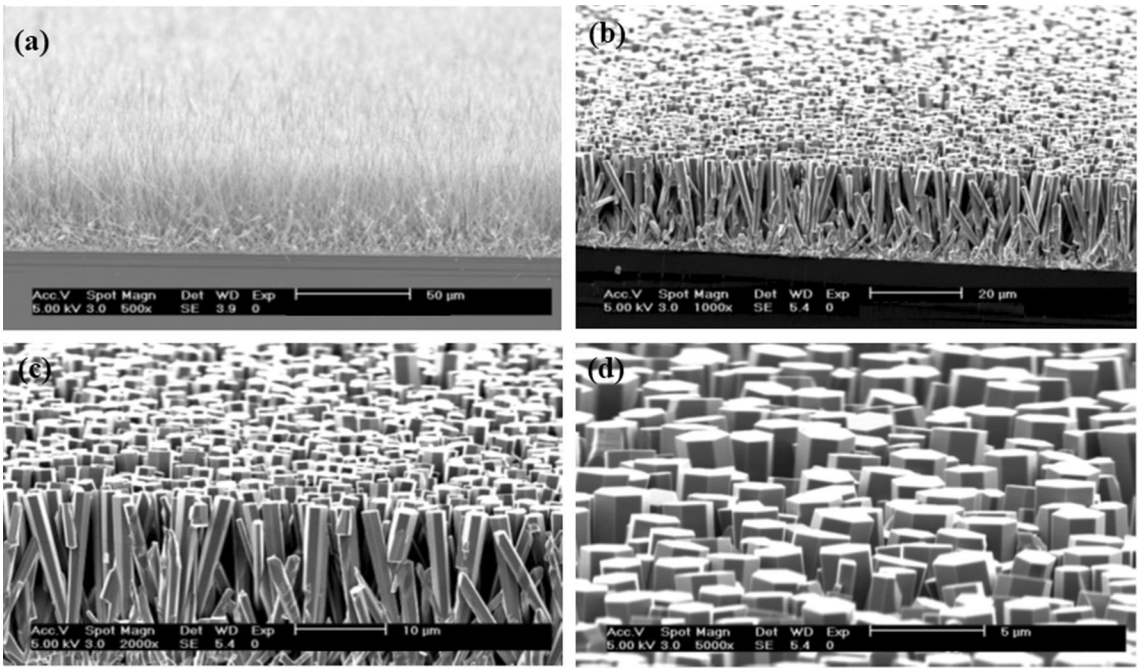

Fig. 1. Cross-sectional and in-plane FESEM image of as-grown ZnO nanorods on Si substrate (a) scale bar: 50 μm (b) scale bar: 20 μm (c) scale bar: 10 μm (d) scale bar: 5 μm.

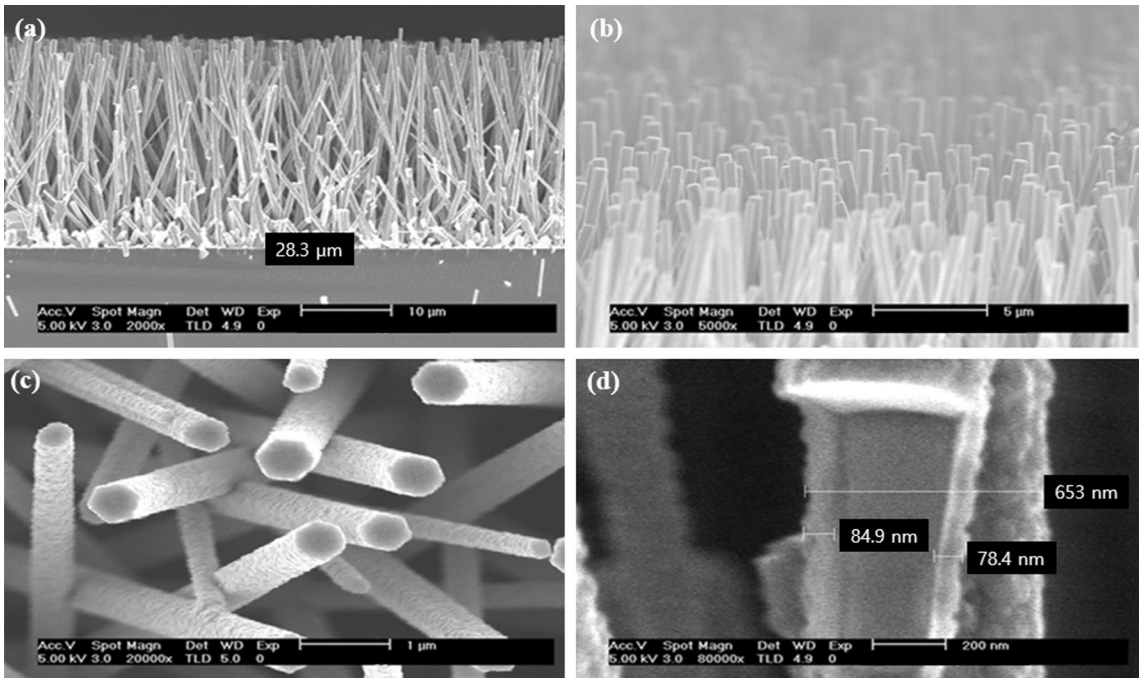

Fig. 2. High-magnification FESEM image of the perpendicularly aligned Si-ZnO coaxial nanorod arrays grown on Si substrate at the Si growing temperature of 500˚C (a) scale bar: 10 μm (b) scale bar: 5 μm (c) scale bar: 1 μm (d) Scale bar: 200 nm (thickness of Si shell: 78–85 nm).

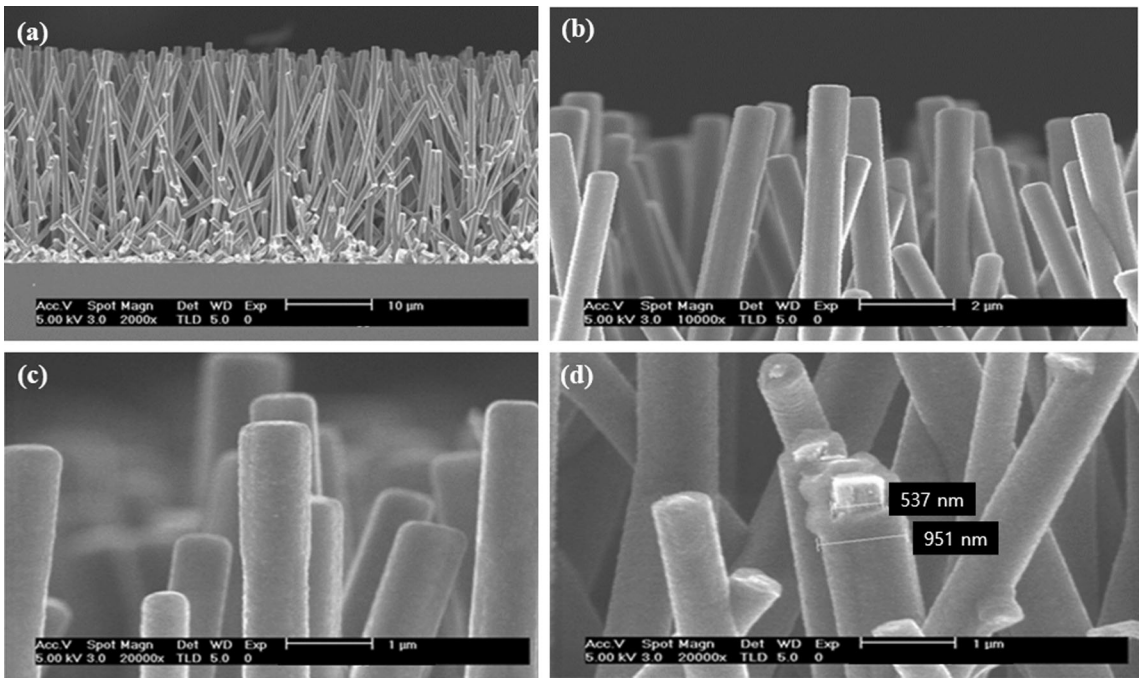

Fig. 3. High-magnification FESEM image of the perpendicularly aligned Si-ZnO coaxial nanorod arrays grown on Si substrate at the Si growing temperature of 600˚C (a) scale bar:10 μm (b) scale bar: 2 μm (c) scale bar: 1 μm (d) scale bar: 1 μm (thickness of Si shell: 207 nm).

layer of 500˚C, 600˚C, 650˚C, and 700˚C. The mean length of the Si@ZnO NRs is ~28 μm. The surface density of NRs is $1 \times 10^9/cm^2$. One can see that the Si@ZnO NRs grew perpendicularly. The Si@ZnO NRs have reliable hexagonal form and uniform bottoms, which are perpendicularly aligned along the c-axis in Figs. 2, 3, 4, and 5. For the Si@ZnO NRs made at Si layer growing temperatures of 500˚C, 600˚C, 650˚C, and 700˚C, a mean diameter of the ZnO nanorod and thickness of Si layer correspond to 255 nm, 537 nm, 478 nm, 359 nm, 78–85 nm, 207 nm, 336 nm, and 372 nm, respectively as shown

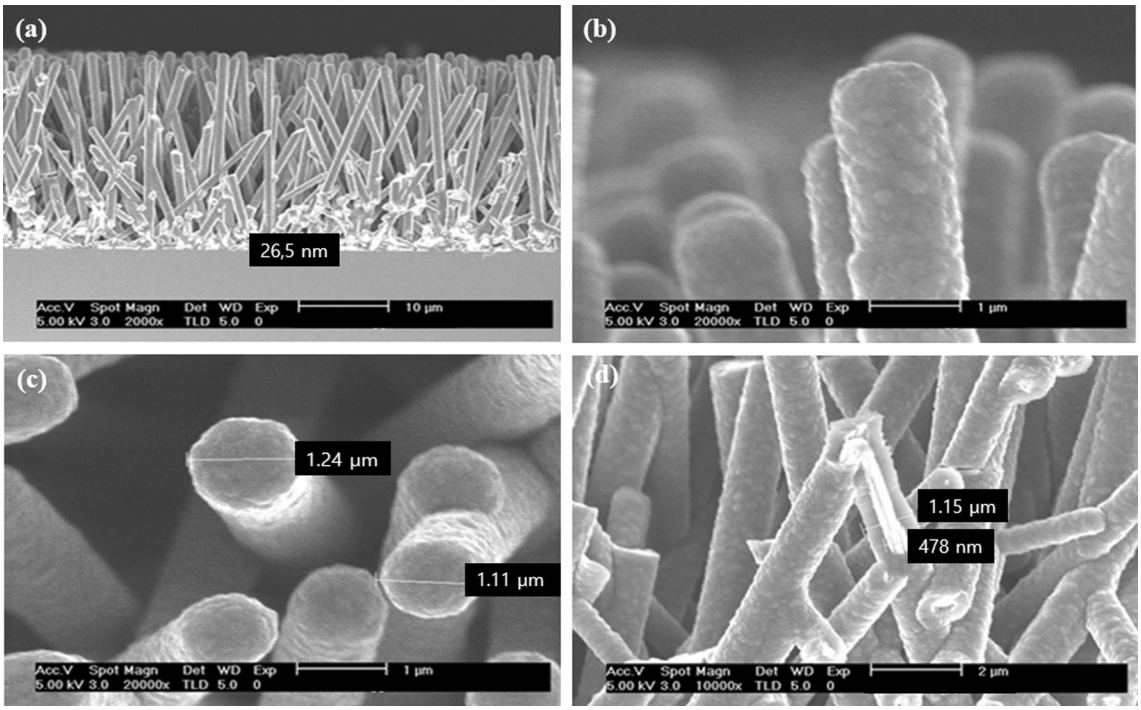

Fig. 4. High-magnification FESEM image of the perpendicularly aligned Si-ZnO coaxial nanorod arrays grown on Si substrate at the Si growing temperature of 650˚C. (a) scale bar: 10 μm (b) scale bar: 1 μm (c) scale bar: 1 μm (d) scale bar: 2 μm (thickness of Si shell: 336 nm).

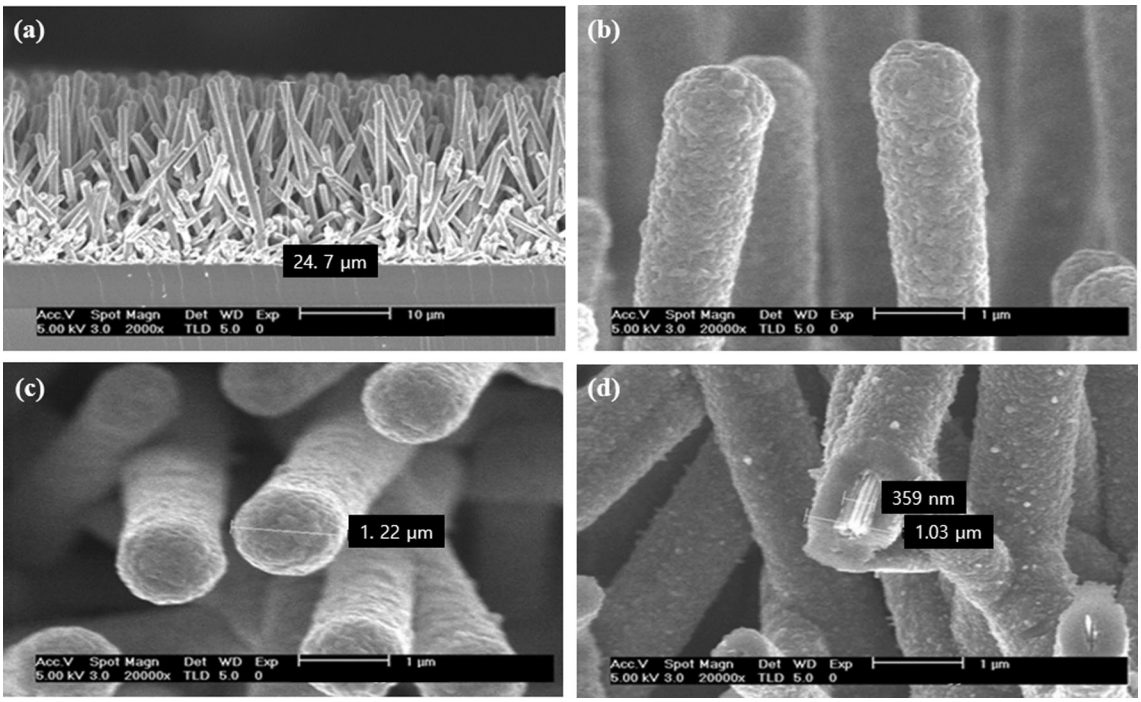

Fig. 5. High-magnification FESEM image of the perpendicularly aligned Si-ZnO coaxial nanorod arrays grown on Si substrate at the Si growing temperature of 700˚C (a) scale bar: 10 μm (b) scale bar: 1 μm (c) scale bar: 1 μm (d) scale bar: 1 μm (thickness of Si shell: 372 nm).

in Figs. 2d, 3d, 4d, and 5d. In previous studies on Si@ZnO NRs made at Si layer growing temperatures of 550˚C, the mean diameter of the ZnO NR and the thickness of Si layer was 330 nm and 103 nm, respectively.[23] Therefore, it could be inferred from the current SEM data and the earlier

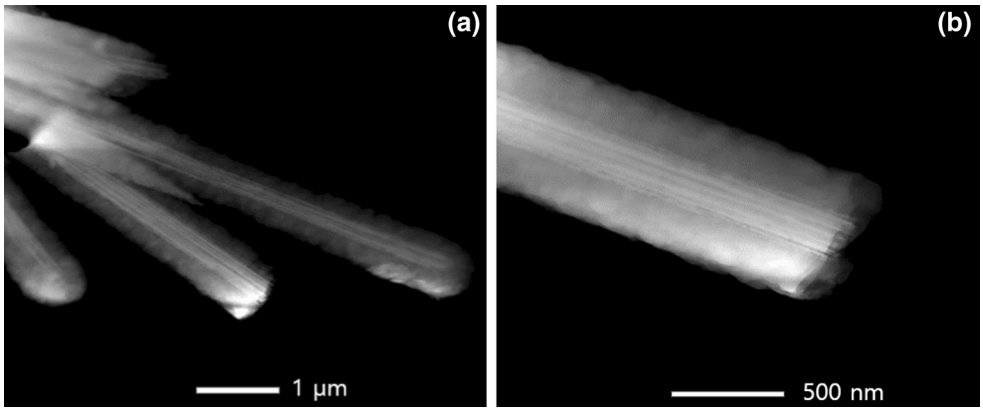

Fig. 6. The HRTEM images of the Si-ZnO coaxial nanorod heterostructure grown on Si substrate at the Si growing temperature of 650˚C (a) scale bar: 1 μm (b) scale bar: 500 nm.

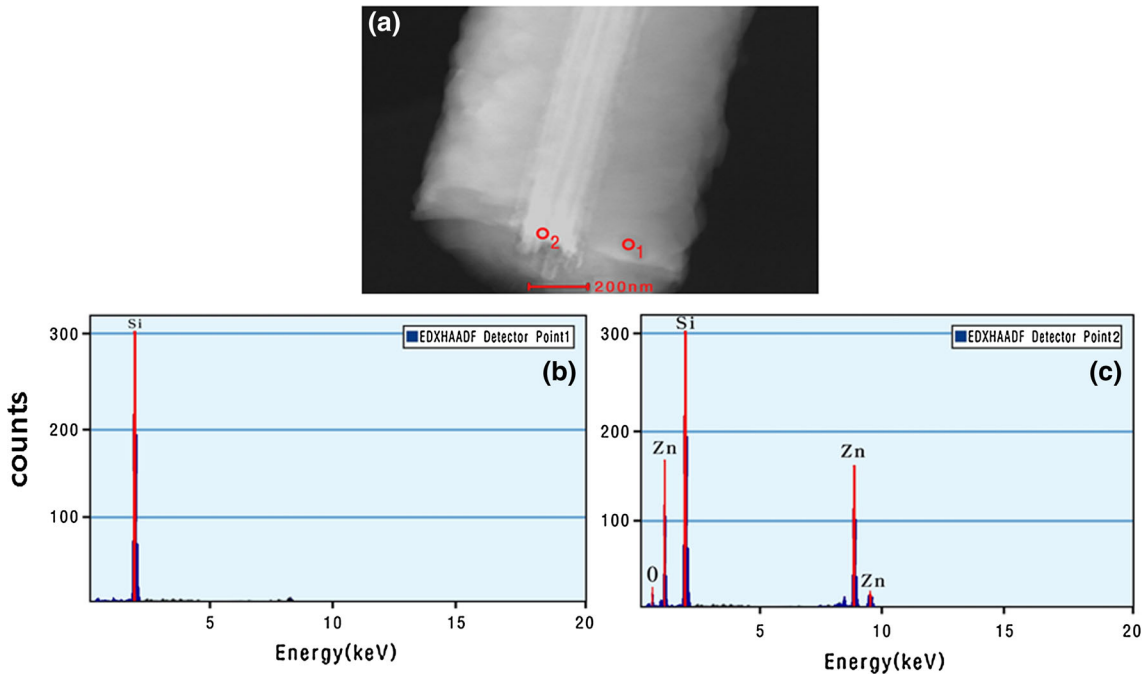

Fig. 7. The EDS spectra of the Si-ZnO coaxial nanorod at a Si growing temperature of 650˚C: (a) HRTEM image of Si-ZnO coaxial nanorod heterostructure (b) EDS spectrum of the Si-ZnO coaxial nanorod heterostructure detected at the point O_1 (c) EDS spectrum of the Si-ZnO coaxial nanorod heterostructure detected at the point O_2.

study that the thickness of the Si layer increases as the Si growth temperatures increase from 500˚C to 700˚C.

Additional fundamental investigation of Si@ZnO NRs made at a Si layer growing temperature of 650˚C was investigated using HRTEM and EDS. As can be seen in Fig. 6a and b, the HRTEM image shows that the Si layer spreads over all the length of the ZnO NR with distinctive intensity at the center and covering layers, which indicates that the Si layer evenly covered the ZnO center NR. The covering was strong and Si layers were not simply stripped off from the ZnO center NR. The difference along the NR outward direction shows bi-axial character. Figure 7a show the HRTEM image of the Si@ZnO NRs at a Si layer growing temperature of 650˚C and Fig. 7b and c shows the typical EDS spectra chosen at the position of O_1 and O_2 of the Si@ZnO NRs made at a Si layer growing temperature of 650˚C. The EDS spectrum chosen at the point O_1 shows that Si layer is constituted of Si. The EDS spectrum chosen at the point O_2 shows that Si@ZnO NRs are composed of Zn, O, Si. The results of the EDS measurements were qualitatively similar for all currently studied samples.

The crystalline structure of the Si@ZnO NRs made at a Si layer growing temperature of 650˚C was examined using XRD, as in Fig. 8. Figure 8 shows the

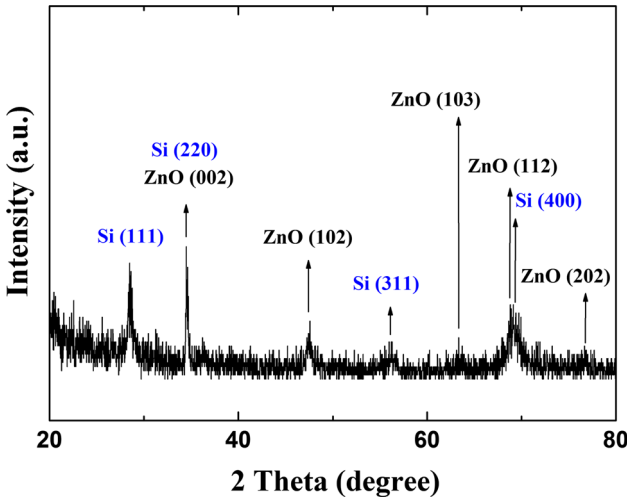

Fig. 8. XRD θ–2θ pattern of Si-ZnO coaxial nanorod heterostructure grown on Si substrate at the Si growing temperature of 650°C which indicate the existence of würtzite ZnO and poly-Si with a zincblende structure.

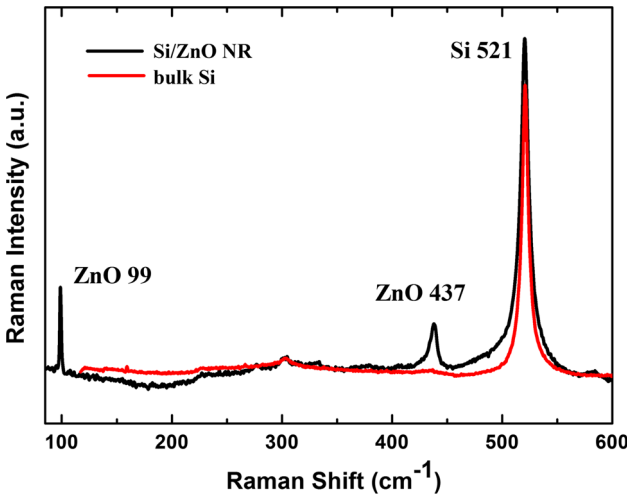

Fig. 9. Typical Raman spectrum (black) obtained from Si-ZnO coaxial nanorod heterostructure grown on Si substrate at the Si growing temperature of 650°C. Raman spectrum (red) corresponds to the bulk Si reference sample (Color figure online).

XRD pattern of the Si@ZnO NRs. The diffraction peaks were assigned to polysilicon with zincblende structure and ZnO with würtzite structure within experimental error, representing that Si@ZnO NRs are composed of Si and ZnO. As can be seen in Fig. 8, center ZnO NRs displayed a main peak at 34.42° assigned to the ZnO (0002) crystal plane. One can see that growing direction of ZnO NR is [0001] from Fig. 8. The peaks observed at $2\theta = 28.5°$, 47.6°, 56.1°, and 69.1° are assigned to (111), (220), (311), and (400) planes of the poly-Si film. It is seen that the Si@ZnO NRs is a compound semiconductor heterostructure of ZnO and silicon with rod appearance based on the SEM and XRD consequences. The a- and c-axis lattice constants estimated from XRD pattern are 3.249 Å and 5.206 Å for ZnO and 5.431 Å for Si, which are in accord with the bulk.[24] The results of the XRD measurements were qualitatively similar for all currently studied samples.

Furthermore, μ-Raman experiment was performed to understand the composition of the Si@ZnO NRs at the growing temperature 650°C of Si layer, and a characteristic Raman spectra is given in Fig. 9. Peak detected at 99 cm^{-1} corresponds to E_2(low) and Peak detected 437 cm^{-1} corresponds to E_2(high) of würtzite ZnO, shifting up to 3 cm^{-1} and 2 cm^{-1} compared to bulk.[25] Observation of E_2 optical-phonon peak shows that the ZnO NRs has the würtzite phase. Along with ZnO peaks, the poly-Si layer displays a strong Si peak at 521 cm^{-1}. A strong Si peak and the nonappearance of an amorphous Si (a-Si) peak show that the crystallinity of the poly-Si layer is outstanding. The appearance of the poly-Si mode shows that the Si NRs is the polysilicon with a zincblende structure, which is in accord with the TEM and XRD results. The Raman features of the Si@ZnO NRs made at the growing temperature of 500°C, 600°C, and 700°C of Si layer are similar to all currently studied samples and those observed for the Si@ZnO NRs made at the growing temperature of 550° C of Si layer.[23] Hence, we confirmed that the poly Si layer was well covered over ZnO single crystal NRs with würtzite structure and well-aligned Si@ZnO NRs were successfully made. The coaxial heterostructures consisting of ZnO NRs (n-type) and Si (p-type) layer as described in this study could make the best use of the intrinsic characteristics of ZnO and Si with increased covering regions and the configuration of Si-ZnO heterojunctions. The Si-ZnO coaxial nanostructures are anticipated to have an advantage in optoelectronic, photonic, and sensing applications such as solar diode sensor and photodiodes which is potentially useful from UV to infrared light sensing.

CONCLUSIONS

We successfully synthesized the Si@ZnO NRs produced at the growing temperature of 500°C, 600° C, 650°C, and 700°C of Si layer and examined the fundamental features of the Si@ZnO NRs at the growing temperatures of 500°C, 600°C, 650°C, and 700°C of Si layer. FESEM revealed that a thickness of Si shell of the Si@ZnO NRs increases with increasing growing temperatures of Si layer from 500°C to 700°C. XRD, EDS, and Raman experiments confirmed that the Si@ZnO NRs were made perpendicularly on semi-insulating (100)-oriented Si substrates and the ZnO NRs was single crystals with a würtzite structure, and the Si layer was polysilicon with a zincblende structure.

ACKNOWLEDGEMENTS

This research was supported by Basic Science Research Program through the National Research Foundation of Korea (NRF) Grant funded by the Ministry of Education, Science and Technology (MEST) (NRF-2014M2B2A4032178), (NRF-2016R1

D1A1B03930992), (NRF-2016R1A6A1A03012877) as well as under the framework of international cooperation program managed by National Research Foundation of Korea (2015K2A1B8068543).

REFERENCES

1. S.W. Jung, W.I. Park, G.C. Yi, and M. Kim, *Adv. Mater.* 15, 1358 (2003).
2. C.H. Lee, J.K. Yoo, Y.J. Doh, and G.C. Yi, *Appl. Phys. Lett.* 94, 043504 (2009).
3. L.J. Lauhon, M.S. Gudiksen, D. Wang, and C.M. Lieber, *Nature* 420, 57 (2002).
4. J. Hu, Y. Bando, Z. Liu, T. Sekiguchi, D. Goldberg, and J. Zhan, *J. Am. Chem. Soc.* 125, 11306 (2003).
5. S.J. An, W.I. Park, G.C. Yi, Y.J. Kim, H.B. Kang, and M.Y. Kim, *Appl. Phys. Lett.* 84, 3612 (2004).
6. Y.J. Hong, J.M. Jeon, M. Kim, S.R. Jeon, K.H. Park, and G. C. Yi, *New J. Phys.* 11, 125021 (2009).
7. W.I. Park, J.K. Yoo, D.W. Kim, G.C. Yi, and M. Kim, *J. Phys. Chem. B Lett.* 110, 1516 (2006).
8. W.I. Park, G.C. Yi, M.Y. Lim, and S.J. Pennycook, *Adv. Mater.* 15, 526 (2003).
9. X.Q. Meng, H. Peng, Y.Q. Gai, and J. Li, *J. Phys. Chem. C* 114, 1467 (2010).
10. K.Q. Peng, X. Wang, X.L. Wu, and S.T. Lee, *Nano Lett.* 9, 3704 (2009).
11. Y. Cui, Q.Q. Wei, H.K. Park, and C.M. Lieber, *Science* 293, 1289 (2001).
12. R.R. He and P.D. Yang, *Nat. Nanotechnol.* 1, 42 (2006).
13. Y. Huang, X.F. Duan, Y. Cui, L.J. Lauhon, K.H. Kim, and C. M. Lieber, *Science* 294, 1313 (2001).
14. J.S. Jie, W.J. Zhang, K.Q. Peng, G.D. Yuan, C.S. Lee, and S. T. Lee, *Adv. Funct. Mater.* 8, 3251 (2008).
15. X. Zhang, X. Zhang, X. Zhang, Y. Zhang, L. Bian, Y. Wu, C. Xie, Y. Han, Y. Wang, P. Gao, L. Wang, and J.S. Jie, *J. Mater. Chem.* 22, 22873 (2012).
16. D. Ma, C.S. Lee, F.C. Au, S.Y. Tong, and S.T. Lee, *Science* 299, l874 (2003).
17. Y. Wu, J. Xiang, C. Yang, W. Lu, and C.M. Lieber, *Nature* 430, 6l (2004).
18. Y. Wu, R. Fan, and P.D. Yang, *Nano Lett.* 2, 83 (2002).
19. C. Wang, J. Wang, Q. Li, and G.C. Yi, *Adv. Funct. Mater.* 75, 1471 (2005).
20. H.S. Song, W.J. Zhang, C. Cheng, Y.B. Tang, L.B. Luo, X. Chen, C.Y. Luan, X.M. Meng, J.A. Zapien, N. Wang, C.S. Lee, I. Bello, and S.T. Lee, *Cryst. Growth Design* 11, 147 (2011).
21. A.E. Gada, M.W.G. Hoffmanna, F. Hernandez-Ramirezb, J. D. Pradesb, H. Shena, and S. Mathura, *Mater. Chem. Phys.* 135, 618 (2012).
22. A.E. Gad, M. Hoffmann, F. Hernandez-Ramirez, J.D. Prades, H. Shen, and S. Mathur, *Procedia Eng.* 47, 1279 (2012).
23. H.D. Cho, H.Y. Cho, D.W. Kwak, T.W. Kang, and I.T. Yoon, *J. Cryst. Growth* 437, 26 (2016).
24. Ü. Özgür, Y.I. Alivov, C. Liu, A. Teke, M.A. Reshchikov, S. Doğan, V. Avrutin, S.J. Cho, and H. Morkoç, *J. Appl. Phys.* 98, 041301 (2005).
25. K.A. Alim, V.A. Fonoberov, M. Shamsa, and A.A. Balandin, *J. Appl. Phys.* 97, 124313 (2005).